

## Article

# Effect of Blending Dimethyl Carbonate and Ethanol with Gasoline on Combustion Characteristics

Shunsuke Suzuki <sup>1,\*</sup>, Eiichi Takahashi <sup>2</sup>, Mitsuharu Oguma <sup>1</sup> and Kazuhiro Akihama <sup>2</sup>

<sup>1</sup> Research Institute for Energy Conversion, National Institute of Advanced Industrial Science and Technology (AIST), 1-2-1 Namiki, Tsukuba 305-8564, Ibaraki, Japan; mitsu.oguma@aist.go.jp

<sup>2</sup> Department of Sustainable Engineering, College of Industrial Technology, Nihon University, 1-2-1, Izumi-cho, Narashino 275-8575, Chiba, Japan; takahashi.eiichi@nihon-u.ac.jp (E.T.); akihama.kazuhiro@nihon-u.ac.jp (K.A.)

\* Correspondence: suzuki-shunsuke.cv@aist.go.jp

**Abstract:** We investigated the effects of blending dimethyl carbonate (DMC) and ethanol with commercial gasoline on combustion characteristics. Our experimental approach involved using a rapid compression and expansion machine (RCEM) to achieve elevated temperatures and pressures. The fuels containing different volumes of oxygenated hydrocarbons were burned at equivalence ratios of 1.0 or 0.7, an initial temperature of 340 K, and initial pressures of 0.10 or 0.05 MPa. To simulate knocking phenomena, we installed a rectangular channel in the combustion chamber of the RCEM and measured the pressure history inside the chamber. By analyzing the pressure history resulting from the end-gas autoignition, we evaluated the combustion duration and maximum pressure amplitude. Blending both oxygenated fuels with gasoline effectively reduced the maximum-pressure amplitude in the end-gas autoignition, with ethanol exhibiting a more pronounced suppression effect compared to DMC in the same volumetric mixing ratio. At an initial pressure of 0.10 MPa, the combustion durations of DMC/gasoline blends showed non-linear behavior, being shorter than those of pure gasoline and DMC and comparable to those of the ethanol/gasoline blends. However, the blending effect of DMC on combustion durations was greatly mitigated when the initial pressure was reduced to 0.05 MPa. Conversely, the combustion durations for ethanol/gasoline blends showed a nearly monotonic reduction with an increase in the ethanol blending ratio at both initial pressures of 0.10 and 0.05 MPa. Finally, we discussed the differential impact of the blending effect of oxygenated hydrocarbons on combustion characteristics.

**Keywords:** gasoline; dimethyl carbonate; ethanol; knocking; combustion duration; blending effect; e-fuel; bio-fuel



**Citation:** Suzuki, S.; Takahashi, E.; Oguma, M.; Akihama, K. Effect of Blending Dimethyl Carbonate and Ethanol with Gasoline on Combustion Characteristics. *Fuels* **2023**, *4*, 441–453. <https://doi.org/10.3390/fuels4040027>

Academic Editor: Nadir Yilmaz

Received: 3 July 2023

Revised: 9 August 2023

Accepted: 24 October 2023

Published: 26 October 2023



**Copyright:** © 2023 by the authors. Licensee MDPI, Basel, Switzerland. This article is an open access article distributed under the terms and conditions of the Creative Commons Attribution (CC BY) license (<https://creativecommons.org/licenses/by/4.0/>).

## 1. Introduction

Because approximately 20% of carbon dioxide (CO<sub>2</sub>) emission is from the transport sector [1], attention on renewable fuels, so-called e-fuels and bio-fuels, which are produced from renewable H<sub>2</sub> and CO<sub>2</sub> and natural sources like biomass, respectively, which could reduce the carbon footprint of transportation, is growing. E-fuels include hydrogen, methane, synthetic hydrocarbon fuels, and oxygen-containing synthetic fuels that are generated based on renewable electricity [2], while biofuels contain methane, biodiesel, furans like 2-methylfuran and 2,5-dimethylfuran, and alcohols such as methanol, ethanol, and butanol [3]. The feasibility and compatibility of liquid e-fuels with existing infrastructure and vehicle technologies have been discussed, and it has been pointed out that oxygenated fuels have detrimental effects on the materials used in the fueling infrastructure when blended at high concentrations [2]. At the same time, techno-economic analyses have been conducted on fuel production [3–6], showing that the synthesis of oxygenated hydrocarbons using CO<sub>2</sub> as a feedstock is considered a preferable method over the synthesis of oxygen-free hydrocarbons from an energy point of view [7]. Numerical assessments

have also indicated that first- and second-generation biofuels generally have lower greenhouse gas emissions than fossil fuels, provided they are produced in the right way [3]. First-generation biofuels are those produced from edible materials such as sugar-based crops, while second-generation biofuels are derived from non-edible materials such as lignocelluloses. Hence, blending oxygenated hydrocarbons with existing fuels, such as gasoline, with low-to-medium concentrations of oxygenated hydrocarbons is a good option for achieving the reduction in CO<sub>2</sub> emissions with the use of existing infrastructure.

Dimethyl carbonate (DMC) is regarded as a promising e-fuel because of its low toxicity, high miscibility with conventional hydrocarbon fuels, absence of C–C bonds, and high oxygen content [8]. The synthesis technology and commercial production process of DMC on the industrial scale have been established for chemical products, where CO<sub>2</sub>, H<sub>2</sub>, and methanol are utilized as the main reactants [5]. According to a review article on life cycle assessment, the global warming impact evaluated by equivalent CO<sub>2</sub> emissions in DMC was comparable to or lower than that of conventional fossil fuels, making DMC attractive from an economic viewpoint [5]. Among the various bio-fuels, ethanol has been extensively produced as both a first- and second-generation bio-fuel due to its well-established production technologies [3,6]. Ethanol has been widely used worldwide as an additive to gasoline because of its octane enhancing properties, high enthalpy of evaporation, broad ignition boundary, and high laminar flame velocity [9–11]. As stated above, previous life cycle assessments have shown that ethanol produced from bio-based materials can generally contribute to the reduction in CO<sub>2</sub> emissions if no land-use change is involved [3].

Considerable efforts have been devoted to investigating the impact of blending oxygenated hydrocarbons with existing hydrocarbons on combustion characteristics. In the case of ethanol/gasoline blends, many combustion studies in engines have consistently shown [9,12–14] improved thermal efficiency and engine power, as well as the reduced emissions of pollutants such as CO, unburned hydrocarbons, and NO<sub>x</sub>. It has been reported that among C<sub>1</sub>–C<sub>5</sub> alcohols, ethanol exhibits the best anti-knock property when blended with gasoline [15]. Laboratory-scale studies have been conducted to explore the influence of ethanol addition to gasoline surrogate components like n-heptane and iso-octane on combustion characteristics [11,16–18]. Although the laminar burning velocities of ethanol/n-heptane and ethanol/iso-octane blends fell between those of pure fuels, they did not show a linear relationship with the blending ratios [9,16]. According to the experiments used to measure the ignition delay time (IDT) of ethanol/iso-octane blends, IDTs increased as ethanol blending ratios decreased in high-temperature regions [17,18], while the IDTs of the blends were longer than those of pure fuel in negative-temperature coefficient regions [17]. Bogin Jr. et al. suggested that this non-linear behavior might be attributed to the non-linearity of the research octane number (RON) in ethanol/iso-octane blends [19]. Although the effect of DMC blending has been less studied compared to ethanol, there are several articles focusing on gasoline engines [13,14,20–22] and fundamental combustion experiments in the laboratory [23–25]. When DMC was blended with gasoline for use in gasoline engines, pollutant emissions were reduced compared to using pure gasoline [13,14,21]. Faster combustion and higher engine efficiency were observed in DMC/gasoline blends under the conditions of lean engine operation [20], while the combustion speed of the blending fuel was nearly equal to or lower than pure gasoline under stoichiometric and rich conditions [14,20]. In premixed n-heptane flame doped with DMC, there was a reduction in the mole fractions of C<sub>1</sub>–C<sub>6</sub> hydrocarbons, and an earlier onset of CO<sub>2</sub> formation compared to pure n-heptane flame was found, which might be attributed to the inherent reaction nature of DMC [23]. IDTs of DMC/n-heptane/oxygen/argon mixtures with different DMC concentrations were lower, with an increase in DMC ratios at temperatures above 1200 K, while the opposite trend was observed at lower temperatures, suggesting that DMC is a promising octane booster [24].

In general, knocking involves high-frequency pressure oscillations associated with the auto-ignition of a portion of the unburned air–fuel mixture ahead of the propagating flame front, and should be suppressed to avoid engine damage and improve thermal

efficiency. One of the methods used to improve anti-knock performance is the utilization of anti-knock additives [10]. Among these additives, oxygenated hydrocarbons have shown a promising anti-knock effect [10,15]. Christensen et al. investigated the anti-knock properties of various oxygenates, such as alcohols, esters, and furans, blended with gasoline, and found that the octane-enhancing effect was strongly dependent on the type of oxygenates: ethanol and furans like 2-methylfuran and 2,5-dimethylfuran were very effective for improving anti-knock capability, while butanols did not enhance knock resistance as much as expected from their octane number, and some oxygenates, such as 1-pentanol and 2-methyltetrahydrofuran, even worsened knock resistance [15]. Ethanol has been widely recognized as a promising octane booster [10,15], while few academic studies have been conducted on the octane-enhancing effect of DMC, despite several patents regarding its use as a gasoline additive up to 10% [26]. Overall, there is a lack of fundamental research on the influence of combustion characteristics related to knocking when DMC is blended at concentrations higher than 10%, and, simultaneously, there has been a fundamental lack of investigation comparing and examining the blending effects of different oxygenated hydrocarbons like ethanol and DMC, despite the fact that a few studies have been conducted on spark-ignited engines [13,14,20].

To bridge a gap present in previous studies, this study aims to reveal the influence on the knocking phenomena when DMC is blended over a wide range, as well as to explore the blending effect of different oxygenated fuels on combustion characteristics, specifically focusing on the knocking intensity resulting from end-gas autoignition and on combustion duration under high-temperature and -pressure conditions similar to engines. For this, DMC or ethanol were blended with commercial gasoline available in Japan. To achieve conditions comparable to those of an engine, a rapid compression and expansion machine (RCEM) located at National Institute of Advanced Industrial Science and Technology (AIST) was utilized, which allowed the authors to conduct experiments without fatal damage to the system, even in the presence of significant pressure oscillations associated with knocking. A rectangular combustion channel was installed within the RCEM chamber to create high-pressure and -temperature conditions, facilitating the end-gas autoignition with good reproducibility. The pressure history inside the chamber was measured to evaluate the maximum pressure amplitude resulting from the end-gas autoignition and the combustion duration. In this study, the maximum pressure amplitude was used as an indicator of knocking strength [27]. The present experimental results revealed different effects on combustion characteristics between DMC and ethanol. Both fuels demonstrated a reduction in knocking. However, the combustion duration of DMC/gasoline blends was shorter than that of pure fuels, whereas such behavior was not found in ethanol/gasoline blends.

## 2. Experiment

In this study, the RCEM, which was placed in AIST and used to assess combustion characteristics in our previous studies [27–30], was used to achieve high-pressure and -temperature conditions. A depiction and specifications of the RCEM used herein are presented in Figure 1 and Table 1, respectively. The piston of the RCEM was driven by hydraulic pressure equipped with feedback control using a computer, according to the measurements of the laser displacement sensors. The piston had a non-lubricated seal to prevent ignition and combustion caused by lubricating oil. The bore and stroke were 100 mm and 120 mm, respectively. The piston top was made of aluminum with a flat and smooth shape. During the measurements, the first piston position was the bottom dead center position, and it then moved to the top dead center position to compress the air–fuel mixtures, and was maintained at the top dead center position for approximately 140 ms. Then, the piston returned to its base position. The flow rates of liquid fuel and air (G3 grade, TAIYO NIPPON SANSO) were adjusted using individual mass flow controllers (Bronkhorst mini CORI-FLOW for liquid fuel and EL-FLOW SELECT for air). Commercial gasoline available in Japan, pure DMC, pure ethanol, and DMC/gasoline and ethanol/gasoline blends with different volume blending ratios were used as liquid fuels.

Properties of DMC/gasoline and ethanol/gasoline are summarized in Tables S1 and S2 in the Supplementary Material. Air–fuel mixtures at atmospheric pressure were prepared using a vaporizer (Bronkhorst CEM, Gelderland, The Netherlands) located posterior to the mass flow controllers. Note that adding oxygenated hydrocarbons results in a reduction in the calorific value per unit volume, which leads to a decrease in output power in actual use if the amount of fuel input is the same. After each measurement, the burned gas was exhausted using a vacuum pump, and the fresh gases were charged. The line from the vaporizer to the combustion chamber was heated to prevent fuel condensation. In addition, the temperatures of the cylinder wall, piston, and window frame were maintained using an electrical heater and hot oil circulation. The experiments under each condition were repeated three times.

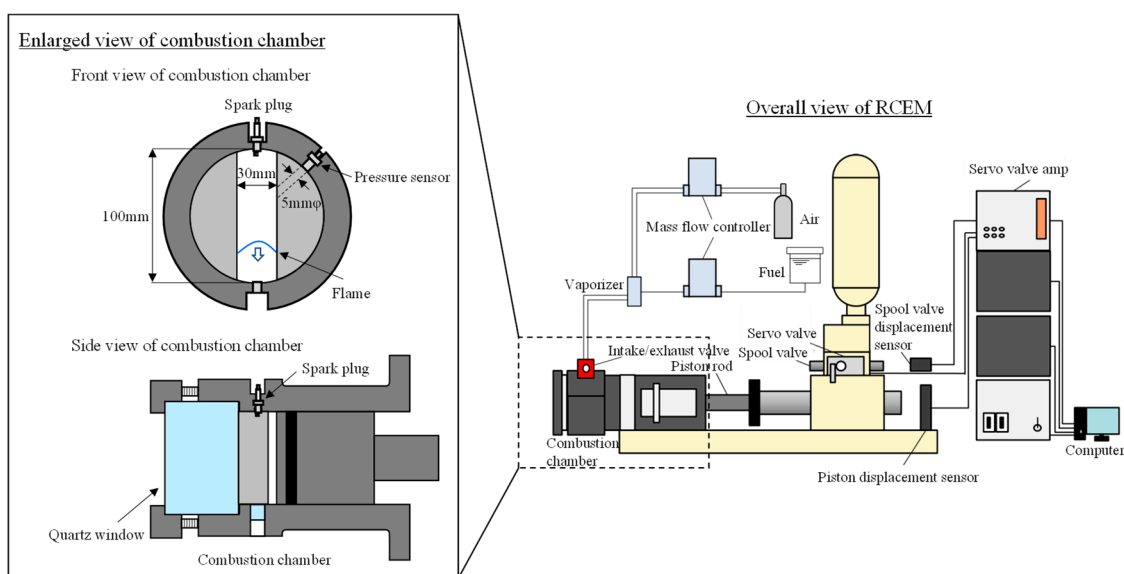


**Figure 1.** Schematic of the RCEM used in this study. Overall view of the RCEM and the enlarged view of combustion chamber.

**Table 1.** Summary of details of the RCEM and experimental conditions in this study.

Bore and stroke	100 mm and 120 mm
Corresponding piston speed	1200 rpm
Compression ratio	7.5
Piston compression velocity	5 m/s
Piston shape	Flat top
Fuel	Gasoline/DMC (DMC: 0, 20, 40, 60, 100 vol.%) Gasoline/ethanol (ethanol: 0, 20, 40, 60, 100 vol.%)
Equivalence ratio	0.7 and 1.0
Initial temperature of chamber	340 K
Initial pressure of chamber	0.05 and 0.10 MPa

To measure the maximum pressure amplitude in the end-gas autoignition, which is a characteristic of the knocking phenomenon, a rectangular combustion channel, identical to that used in our previous study [27], was installed in the cylinder of the RCEM. The detailed dimensions of the rectangular channel can be seen in Figure 1. The pressure history was measured using a pressure sensor (QD34D, AVL) placed on the combustion chamber. The air–fuel mixtures were ignited by a spark plug located at the top of the rectangular channel after the compression was completed by a piston. During the movement of the

piston, a strong squish flow from the gap between the channel and piston, which often induces turbulent flow, was created. After ignition, the flame propagated downward toward the end-gas region, which was located between the flame and chamber wall. Eventually, auto-ignition of the end-gas took place, with the time depending on the fuels. The pressure oscillation induced by autoignition was determined based on the pressure history monitored using a pressure sensor, as described previously [27]. The knocking index (KI) was used to represent the intensity of the knocking phenomena. KI is defined in the following equation,

$$KI = \max(|p_{HPF}|) \quad (1)$$

where  $p_{HPF}$  represents filtered pressure histories above 2 kHz. High-frequency components higher than 2 kHz were transformed from the measured pressure history using Fourier transformation. A threshold frequency of 2 kHz was adopted to exclude pressure oscillations originating from the background. KI was defined as the difference between the maximum and minimum pressures of the high-frequency component. The air–fuel mixtures were supplied to a chamber at equivalence ratios of 0.7 or 1.0. We selected equivalence ratio of 1.0 because stoichiometric conditions are usually employed in an actual gasoline engine with port-injection. Equivalence ratio of 0.7 was employed as a representative of lean conditions. The initial temperature was set at 340 K, and the initial pressure in the combustion chamber was 0.10 MPa or 0.05 MPa. We assumed that the minimum pressure after compression and the peak pressure after combustion were comparable to 0% and 100% of mass fraction burned, respectively. The heat release rate ( $dQ/dt$ ) under the ideal gas assumption can be expressed by the following equation, which is analogous to the engine environment [31]:

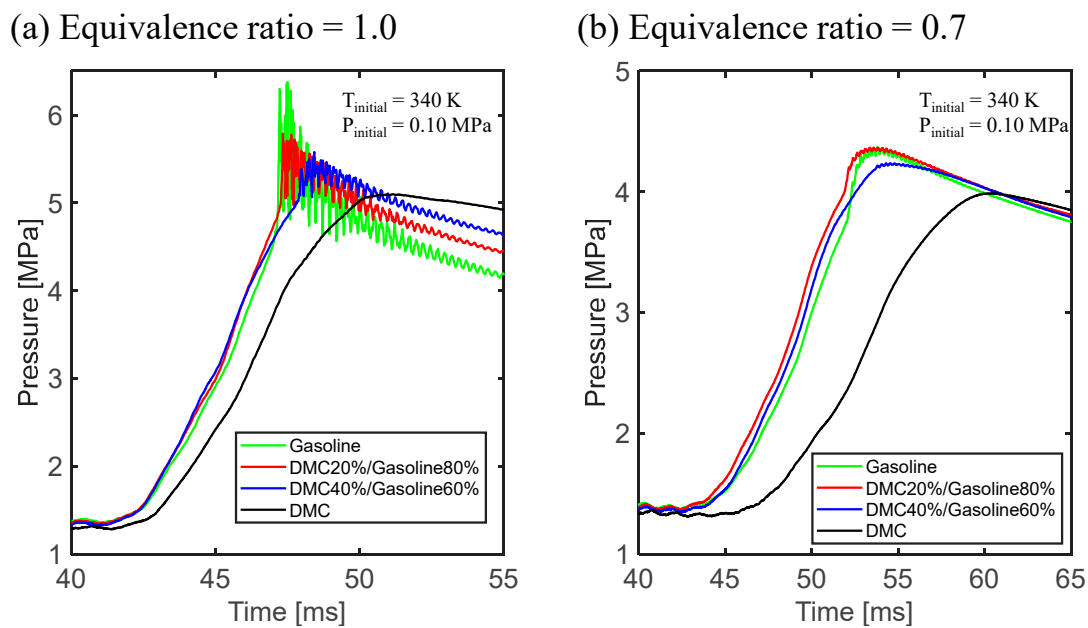
$$\frac{dQ}{dt} = \frac{\gamma}{\gamma - 1} p \frac{dV}{dt} + \frac{1}{\gamma - 1} V \frac{dp}{dt} \quad (2)$$

where  $\gamma$  is the ratio of the specific heat. Because  $dV/dt$  is zero in the present RCEM and  $dp/dt$  is zero at the minimum and maximum pressures,  $dQ/dt$  becomes zero when the mass fraction burned is equal to 0% and 100%. Here, we defined two characteristic times:  $\tau_d$ , which is defined as the duration time from the start of the ignition (40 ms) to 10% of the mass fraction burned in a cylinder, and  $\tau_b$ , which is defined as the duration time from 10% to 50% of the mass fraction burned. The duration time from 10% to 50% of the mass fraction burned is adopted here instead of that from 10% to 90% of the mass fraction burned in order to avoid the influence of knocking.  $\tau_d$  and  $\tau_b$  correspond to the flame development and main burning durations, respectively [32].

### 3. Results and Discussions

#### 3.1. Experimental Results

The pressure histories in DMC/gasoline blends at an initial pressure of 0.10 MPa are given in Figure 2. After ignition is initiated at 40 ms, the pressure increases owing to end-gas autoignition. In Figure 2, the green, red, blue, and black lines represent the pressure profiles attributed to gasoline, DMC20%/gasoline80%, DMC40%/gasoline60%, and DMC, respectively. At an equivalence ratio of 1.0 (Figure 2a), although the intense pressure oscillation takes place in pure gasoline, it is mitigated as an increase in the blending ratio of DMC. When equivalence ratio decreases to 0.7, the intense knocking does not occur, but the slight pressure oscillation can be found in gasoline and DMC20%/gasoline80% fuel. Similarly to the case of equivalence ratio of 1.0, the pressure oscillations at equivalence ratio of 0.7 can be mitigated with an increase in DMC blending ratio. It is noteworthy that in Figure 2, the onset of pressure rise in DMC/gasoline blends is slightly earlier than that in pure gasoline and DMC. In this study, the onset of pressure rise was defined as the time when the rate of change in pressure varied from negative to positive. This tendency is observed at both equivalence ratios, but the impact of DMC blending on this is more pronounced at an equivalence ratio of 0.7 than at an equivalence ratio of 1.0.



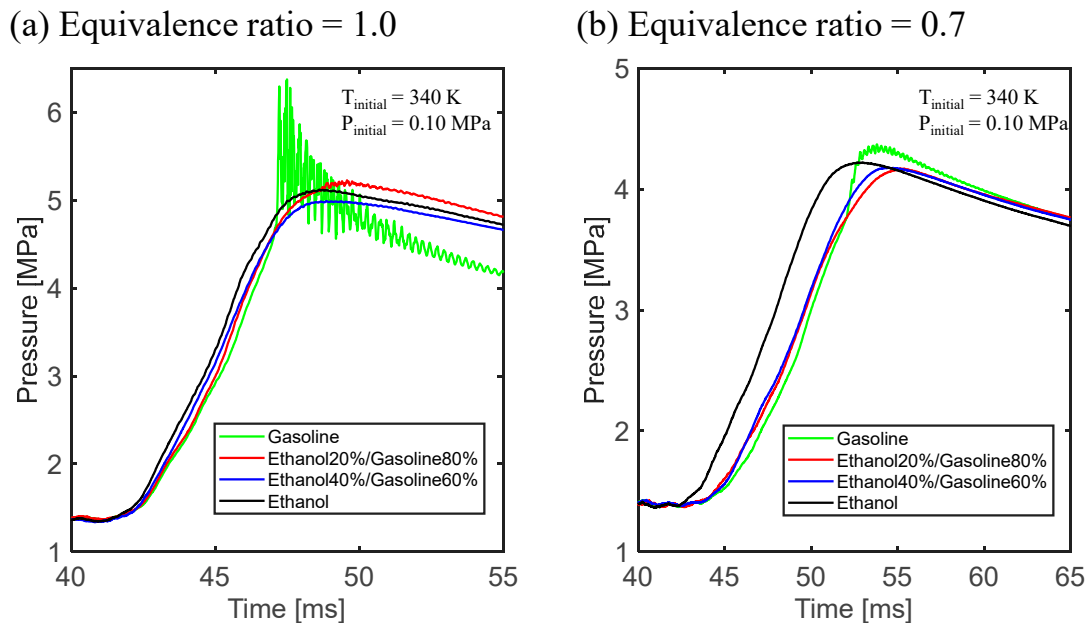
**Figure 2.** Pressure histories in gasoline/air, DMC/air, and DMC/gasoline/air mixtures at equivalence ratios of (a) 1.0 and (b) 0.7. Initial temperature and initial pressure were 340 K and 0.10 MPa, respectively. The pressure histories were described based on the average of trials.

Figure 3 illustrates the pressure histories in ethanol/gasoline blends under a similar condition in DMC/gasoline blends. The pressure profiles of gasoline, ethanol20%/gasoline80%, ethanol40%/gasoline60%, and ethanol are represented by the green, red, blue, and black lines, respectively. In both equivalence ratios, ethanol addition is highly effective for a reduction in the pressure oscillations resulting from knocking. While pressure oscillations are observed at DMC blending ratios of 20% and 40% (Figure 2), they hardly occur in ethanol/gasoline blends with a blending ratio above 20%, as shown in Figure 3. In contrast to DMC blending, the onset of pressure rise in ethanol/gasoline blends occurs earlier, as the ethanol blending ratio increases at both equivalence ratios. It is important to note that no knocking takes place even in pure gasoline when the initial pressure is reduced to 0.05 MPa, although these data are not presented here. However, the blending effect on the onset of the pressure rise, which corresponds to the start of combustion, could be found to some degree at this pressure, as discussed later.

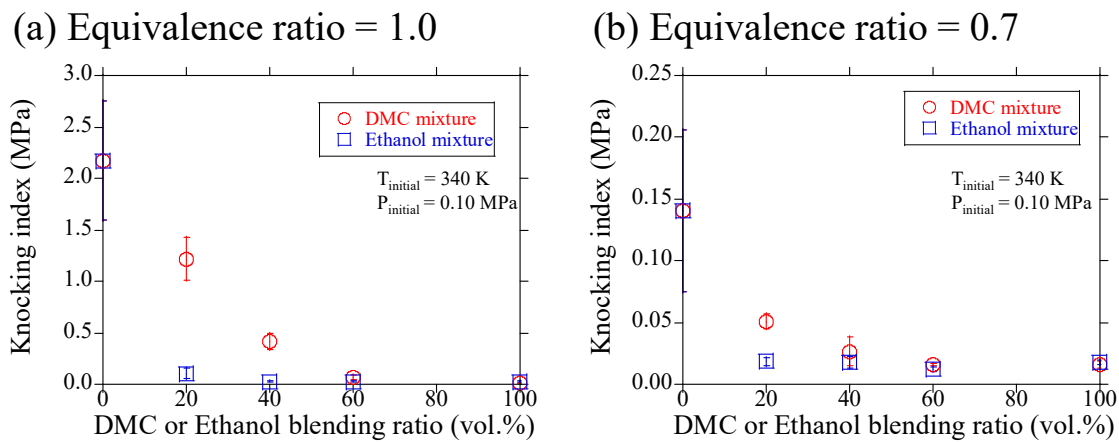
To visualize the intensity of pressure oscillations, Figure 4 displays KI under stoichiometric and lean conditions as a function of DMC and ethanol blending ratios. The error bars in the figure are determined based on the deviation standard in the trials. As observed in the pressure profiles, KI is significantly reduced by the addition of both DMC and ethanol under both equivalence ratios. From Figure 4a, it can be found that knocking is rarely present at DMC and ethanol blending ratios above 60 vol.% and 20 vol., respectively. This indicates that ethanol exhibits greater resistance to knocking when mixed with gasoline at the same mixing volume. This trend seen under stoichiometric conditions is also applicable to an equivalence ratio of 0.7, as demonstrated in Figure 4b.

Figure 5 displays the two characteristic times,  $\tau_d$  and  $\tau_b$ , of stoichiometric air–fuel mixtures at an initial pressure of 0.10 MPa as a function of DMC and ethanol blending ratios. The error bars in the figure represent the deviation standard in the trials. In DMC/gasoline blends, both characteristic times show a convex downward trend. Notably,  $\tau_d$  and  $\tau_b$  at 20 and 40 vol.% are lower than those of the parent fuels. This is consistent with the tendency observed in the pressure profiles in Figure 2, and is intriguing because the characteristic times of pure DMC are the lowest among the fuels examined. This result suggests that the flame speed is enhanced by blending DMC up to 40 vol.%. On the other hand, in ethanol/gasoline blends,  $\tau_d$  and  $\tau_b$  decrease as the ethanol blending ratio increases up to

40 vol.%, and a further increase in the ethanol blending ratio results in nearly constant values for both characteristics times.



**Figure 3.** Pressure histories in gasoline/air, ethanol/air, and ethanol/gasoline/air mixtures at equivalence ratios of (a) 1.0 and (b) 0.7. Initial temperature and initial pressure were 340 K and 0.10 MPa, respectively. The pressure histories were described based on the average of trials.



**Figure 4.** Variation in KI as a function of DMC and ethanol blending ratios with gasoline at equivalence ratios of (a) 1.0 and (b) 0.7. Initial temperature and initial pressure were 340 K and 0.10 MPa, respectively.

The variation in  $\tau_d$  and  $\tau_b$  at an equivalence ratio of 0.7 and an initial pressure of 0.10 MPa is presented in Figure 6. The absolute values of both  $\tau_d$  and  $\tau_b$  are generally lower at an equivalence ratio of 0.7 compared to an equivalence ratio of 1.0. However, DMC blending under lean conditions led to a reduction in the characteristic times. Conversely, ethanol mixing results in a nearly monotonic decrease in both characteristic times as an increase in the ethanol blending ratio. These tendencies observed in DMC/gasoline and ethanol/gasoline blends under lean conditions are similar to those under stoichiometric conditions. It is interesting to note in Figures 5 and 6 that the combustion durations of DMC/gasoline blends are comparable to those of ethanol/gasoline blends at the blending ratio up to 40 vol.%, while a further increase in the blending ratio results in a shorter combustion duration in ethanol/gasoline blends compared to DMC/gasoline blends. The results obtained at an initial pressure of 0.10 MPa imply that DMC serves as a flame

accelerator in the mixing fuels, influencing both flame development and burning durations in both stoichiometric and lean environments.

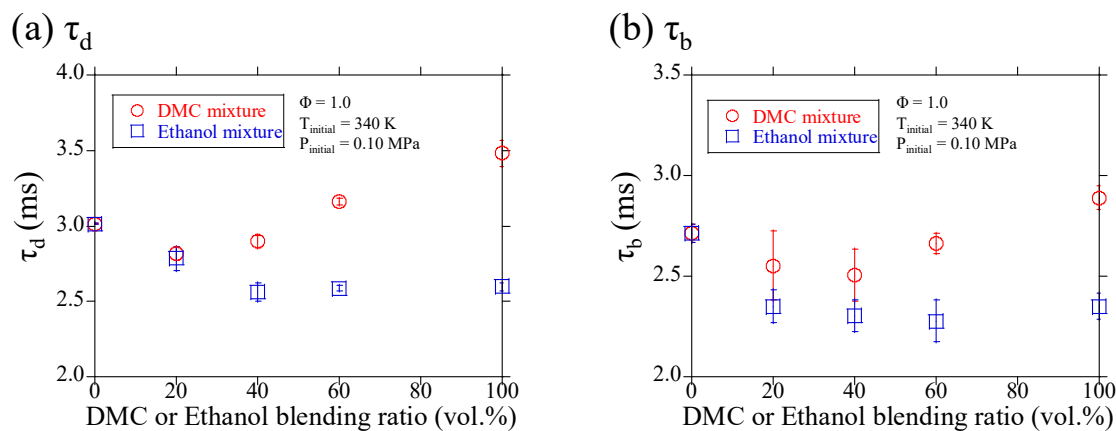


**Figure 5.** Variation in two characteristic times, (a)  $\tau_d$  and (b)  $\tau_b$ , as a function of DMC and ethanol blending ratios with gasoline at an equivalence ratio of 1.0, initial temperature of 340 K, and initial pressure of 0.10 MPa.

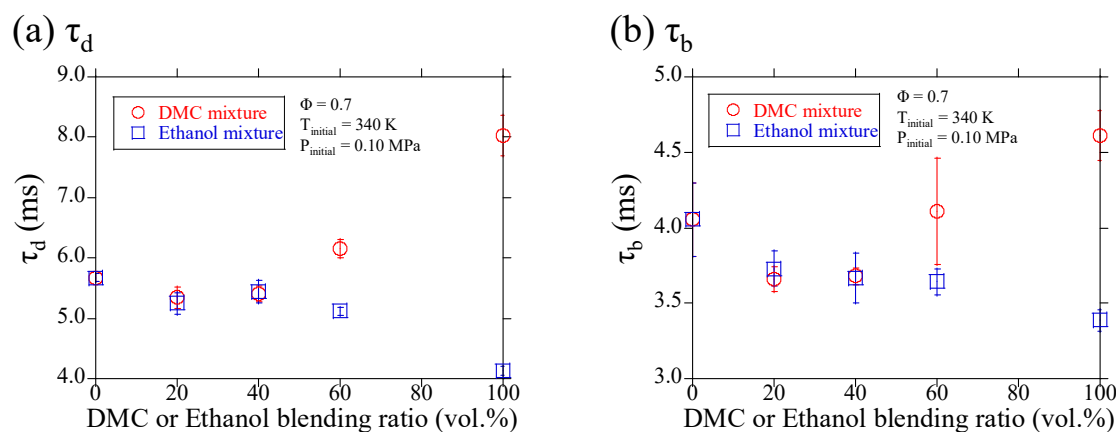


**Figure 6.** Variation in two characteristic times, (a)  $\tau_d$  and (b)  $\tau_b$ , as a function of DMC and ethanol blending ratios with gasoline at an equivalence ratio of 0.7, initial temperature of 340 K, and initial pressure of 0.10 MPa.

The characteristic times in the case of an initial pressure of 0.05 MPa are provided in Figures 7 and 8. Figure 7 shows  $\tau_d$  and  $\tau_b$  at an equivalence ratio of 1.0 and an initial pressure of 0.05 MPa when DMC and ethanol blending ratios are varied. Unlike the experiments at an initial pressure of 0.10 MPa, both times in Figure 7 exhibit an increasing trend with increasing DMC blending ratio. On the other hand, Figure 7 demonstrates that  $\tau_d$  in ethanol/gasoline blends is nearly constant up to 60%, and then decreases with a further increase in the ethanol blending ratio, while  $\tau_b$  in ethanol/gasoline blends is almost constant in every blending ratio. The results at an equivalence ratio of 0.7 and an initial pressure of 0.05 MPa depend on  $\tau_d$  and  $\tau_b$ , as shown in Figure 8. In DMC/gasoline blends,  $\tau_d$  monotonically increases with an increase in DMC blending ratio, while the variation in  $\tau_b$  shows a convex downward shape, although the error bars overlap with each other. The experimental tendency that blending DMC promotes combustion under lean conditions is consistent with that observed in spark-ignited engine [20]. In the case of ethanol/gasoline blends, Figure 8 demonstrates that both times tend to decrease with an increase in the ethanol blending ratio. Comparing the experimental results at initial pressures of 0.10 MPa and 0.05 MPa, the DMC blending effect as a role of a flame accelerator becomes more prominent with an increase in pressure, while the ethanol blending effect that results in a

reduction in the combustion durations with an increase in ethanol blending ratio is nearly independent of pressure.

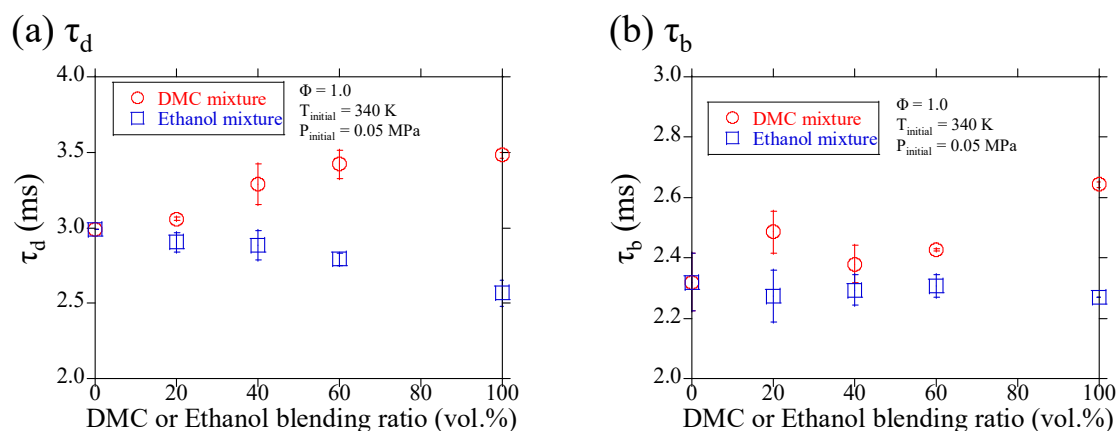


**Figure 7.** Variation in two characteristic times, (a)  $\tau_d$  and (b)  $\tau_b$ , as a function of DMC and ethanol blending ratios with gasoline at an equivalence ratio of 1.0, initial temperature of 340 K, and initial pressure of 0.05 MPa.

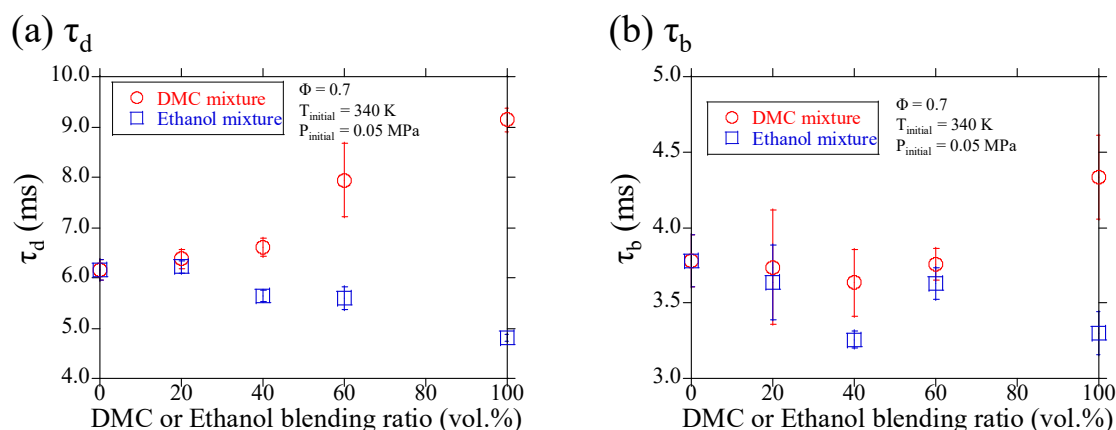


**Figure 8.** Variation in two characteristic times, (a)  $\tau_d$  and (b)  $\tau_b$ , as a function of DMC and ethanol blending ratios with gasoline at an equivalence ratio of 0.7, initial temperature of 340 K, and initial pressure of 0.05 MPa.

### 3.2. Discussions

Through the presented experiments, we succeeded in gaining new insights into the blending effects of ethanol and DMC on knocking intensity and combustion durations. As for knocking intensity, the knock-inhibiting effects of DMC and ethanol were confirmed over a wide range of mixing ratios, as shown in Figure 4, with ethanol being more effective in the same volume ratio. The RON and motor octane number (MON) of DMC are 109–111 and 95–102, respectively [26], while the RON and MON of ethanol are 108–108.5 and 90.7, respectively [19]. Because the RON and MON of pure gasoline are generally lower than those of DMC and ethanol, the reduction in KI by adding DMC and ethanol is considered reasonable due to the increased anti-knock capability of the fuel mixtures. From a combustion chemistry perspective, fuel autoignition, especially knocking, which is closely correlated with low- to intermediate-temperature oxidation mechanisms, has been studied [33–35]. In the case of ethanol, the primary oxidation pathway at low to intermediate temperatures involves hydrogen abstraction at the secondary carbon ( $\alpha$ -position), followed by the addition of oxygen to form peroxy radicals, and then the decomposition of peroxide into formaldehyde and an OH radical [33]. Ethanol oxidation tends to consume free radicals and to prevent the development of a radical pool, leading to a significant reduction in overall reactivity [33,35]. Hence, even when blended with

gasoline in small quantities, ethanol effectively suppresses the low-temperature reactivity of gasoline, resulting in the inhibition of autoignition. The low- to intermediate-temperature oxidation of DMC is mainly initiated by hydrogen abstraction at the  $\alpha$ -position [36], and the subsequent decomposition eventually produces formaldehyde, CO, CO<sub>2</sub>, and a methyl radical. This reaction pathway differs from the low temperature oxidation found in n-alkanes, and the oxygen present in the DMC molecule does not contribute to the formation of reactive radicals [34,35]. As a result, DMCs are probably able to act as an anti-knocking agent when blended with gasoline. In both oxidation processes involving DMC and ethanol, hydrogen abstraction is one of the key reactions, as stated above. The C–H bond dissociation energies (BDE) of ethanol at the  $\alpha$ - and  $\beta$ -sites are 96–98 kcal/mol and 98–100 kcal/mol, respectively [37], while C–H BDE of DMC is 101 kcal/mol [38]. The  $\alpha$ -site C–H BDE of ethanol is the lowest, indicating that radical consumption reactions are more likely to occur. The difference in KI behavior between DMC and ethanol blends shown in Figure 4 may be attributed to the difference in C–H BDE between DMC and ethanol affecting the overall oxidation processes.

Regarding combustion durations, we observed that characteristic times in DMC/gasoline blends were shorter than those of neat fuels and comparable to those of ethanol/gasoline blends, depending on the blending ratio, while ethanol/gasoline blends showed a nearly linear behavior. These trends were more noticeable at an initial pressure of 0.10 MPa compared to 0.05 MPa. Previous investigations on ethanol/n-heptane [11], ethanol/iso-octane [11,39], and ethanol/gasoline [40] blends showed an increase in laminar burning velocity with an increase in the ethanol blending ratio, potentially leading to the shortened combustion duration in ethanol blended fuels. As stated in the experimental section, turbulent flow occurs in the chamber of the RCEM owing to strong squish flow. Considering the close correlation between laminar and turbulent burning velocity [41], our findings of reduced combustion duration with increasing ethanol blending ratio in ethanol/gasoline mixtures seem reasonable. In other words, the behavior of ethanol/gasoline blends is predictable to some degree. On the other hand, as we cannot find specific reports on the blending effect of DMC on both laminar and turbulent burning velocity, the behavior of DMC/gasoline blends is not entirely able to be predicted. Nevertheless, several studies may provide valuable insights for explaining the behavior of combustion duration in DMC/gasoline blends. Flame instability is one of contributing factors to a shortened combustion duration. In some fuel mixtures, such as hydrogen/iso-octane [42], methane/iso-octane [43], compressed natural gas/iso-octane [43], and methane/primary reference fuel (PRF) [44], flame instability was promoted in blends, depending on the equivalence ratios. Flame instability is generally assessed using physical parameters, such as the Markstein length and Markstein number, which showed convex upward or downward trends with respect to the mixing ratio in the aforementioned mixtures [42–44]. These physical quantities are closely related to flame instability, which itself stems from diffusional thermal properties. It is reasonable to assume that the non-monotonic changes in diffusional thermal properties observed in these mixtures are attributed to the mixing of light gases such as hydrogen and methane with heavier gases like iso-octane and PRF. On the other hand, it is plausible to assume that the diffusional thermal properties are not significantly affected in DMC/gasoline blends because of the relatively similar molecular weights of the components. Hence, we have to confirm and verify this assumption, as well as other factors contributing to flame instability, such as hydrodynamic instability, but this is a future task for us that extends beyond the scope of this study. The experimental results obtained here provide a starting point for future investigations, and further extensive studies are required to fully assess the practicality and viability of using DMC/gasoline and ethanol/gasoline blends for internal combustion engines.

#### 4. Conclusions

In this study, the RCEM was used to examine the combustion characteristics of DMC/gasoline and ethanol/gasoline blends. By measuring the pressure histories dur-

ing combustion, knocking intensity and combustion duration were evaluated. Through this work, we successfully obtained new insights into combustion characteristics related to knocking intensity and combustion duration in DMC/gasoline and ethanol/gasoline blends. The results demonstrated that knocking was effectively suppressed by mixing both DMC and ethanol with gasoline, with ethanol showing a greater effectiveness on a volume basis. When 40% DMC or ethanol was blended with gasoline under stoichiometric conditions, KI was reduced by approximately 81% in the DMC mixture and by 99% in the ethanol mixture. While both DMC and ethanol have high anti-knock properties, the difference in the chemical reaction mechanisms of their oxidation processes may be responsible for the difference in knocking mitigation observed in this study. Regarding combustion duration, the behavior differed between DMC/gasoline and ethanol/gasoline blends. The variation in combustion durations in DMC/gasoline blends showed a convex downward tendency, indicating that mixing DMC promoted combustion. This effect was more pronounced at an initial pressure of 0.10 MPa compared to 0.05 MPa. Although the combustion duration of pure DMC was observed to be longer than that of pure ethanol, the combustion duration of DMC/gasoline blends was comparable to that of ethanol/gasoline blends, depending on the experimental conditions. Conversely, the variation in combustion durations in ethanol/gasoline blends was nearly linear with the blending ratio of ethanol at both initial pressures. The behavior of combustion duration in ethanol/gasoline blends was suggested to be partially explained by laminar burning velocity, while that of DMC/gasoline blends could not simply be predicted, presumably due to the non-linear behavior of flame instability or other factors, but this assumption should be confirmed and verified in the future.

**Supplementary Materials:** The following supporting information can be downloaded at: <https://www.mdpi.com/article/10.3390/fuels4040027/s1>, Table S1: Properties of DMC/gasoline blends.; Table S2: Properties of ethanol/gasoline blends.

**Author Contributions:** Conceptualization, E.T.; Methodology, E.T.; Formal Analysis, S.S. and E.T.; Investigation, S.S. and E.T.; Data Curation, S.S. and E.T.; Writing—Original Draft Preparation, S.S.; Writing—Review & Editing, E.T., M.O. and K.A.; Project Administration, M.O.; Funding Acquisition, M.O. All authors have read and agreed to the published version of the manuscript.

**Funding:** The New Energy and Industrial Technology Development Organization (NEDO), Japan.

**Data Availability Statement:** All the data included in this study is presented in the manuscript.

**Acknowledgments:** Special thanks to Koichi Kinoshita (AIST), Yoshinaka Takeda (AIST), and Daiki Asakawa (AIST) for their support.

**Conflicts of Interest:** There are no known competing financial interests or personal relationships that influenced the work reported in this study.

## References

1. *BP Energy Outlook*, 2020 ed.; BP: London, UK, 2020.
2. Ramirez, A.; Sarathy, S.M.; Gascon, J. CO<sub>2</sub> derived E-fuels: Research trends, misconceptions, and future directions. *Trends Chem.* **2020**, *2*, 785–795. [[CrossRef](#)]
3. Jeswani, H.K.; Chilvers, A.; Azapagic, A. Environmental sustainability of biofuels: A review. *Proc. R. Soc. A* **2020**, *476*, 20200351. [[CrossRef](#)] [[PubMed](#)]
4. Pérez-Fortes, M.; Schöneberger, J.C.; Boulamanti, A.; Tzimas, E. Methanol synthesis using captured CO<sub>2</sub> as raw material: Techno-economic and environmental assessment. *Appl. Energy* **2016**, *161*, 718–732. [[CrossRef](#)]
5. Artz, J.; Müller, T.E.; Thenert, K.; Kleinekorte, J.; Meys, R.; Sternberg, A.; Bardow, A.; Leitner, W. Sustainable Conversion of Carbon Dioxide: An Integrated Review of Catalysis and Life Cycle Assessment. *Chem. Rev.* **2018**, *118*, 434–504. [[CrossRef](#)]
6. Zabed, H.; Sahu, J.N.; Boyce, A.N.; Faruq, G. Fuel ethanol production from lignocellulosic biomass: An overview on feedstocks and technological approaches. *Renew. Sustain. Energy Rev.* **2016**, *66*, 751–774. [[CrossRef](#)]
7. Saeidi, S.; Najari, S.; Hessel, V.; Wilson, K.; Keil, F.J.; Concepción, P.; Suib, S.L.; Rodrigues, A.E. Recent advances in CO<sub>2</sub> hydrogenation to value-added products—Current challenges and future directions. *Prog. Energy Combust. Sci.* **2021**, *85*, 100905. [[CrossRef](#)]

8. Abdalla, A.O.G.; Liu, D. Dimethyl Carbonate as a Promising Oxygenated Fuel for Combustion: A Review. *Energies* **2018**, *11*, 1552. [[CrossRef](#)]
9. Manzetti, S.; Andersen, O. A review of emission products from bioethanol and its blends with gasoline. Background for new guidelines for emission control. *Fuel* **2015**, *140*, 293–301. [[CrossRef](#)]
10. Badia, J.H.; Badia, J.H.; Ramírez, E.; Bringué, R.; Cunill, F.; Delgado, J. New Octane Booster Molecules for Modern Gasoline Composition. *Energy Fuels* **2021**, *35*, 10949–10997. [[CrossRef](#)]
11. van Lipzig, J.P.J.; Nilsson, E.J.K.; de Goey, L.P.H.; Konnov, A.A. Laminar burning velocities of n-heptane, iso-octane, ethanol and their binary and tertiary mixtures. *Fuel* **2011**, *90*, 2773–2781. [[CrossRef](#)]
12. Awad, O.I.; Mamat, R.; Ibrahim, T.K.; Hammid, A.T.; Yusri, I.M.; Hamidi, M.A.; Humada, A.M.; Yusop, A.F. Overview of the oxygenated fuels in spark ignition engine: Environmental and performance. *Renew. Sustain. Energy Rev.* **2018**, *91*, 394–408. [[CrossRef](#)]
13. Wen, L.-B.; Xin, C.-Y.; Yang, S.-C. The effect of adding dimethyl carbonate (DMC) and ethanol to unleaded gasoline on exhaust emission. *Appl. Energy* **2010**, *87*, 115–121. [[CrossRef](#)]
14. Schifter, I.; González, U.; Díaz, L.; Sánchez-Reyna, G.; Mejía-Centeno, I.; González-Macías, C. Comparison of performance and emissions for gasoline-oxygenated blends up to 20 percent oxygen and implications for combustion on a spark-ignited engine. *Fuel* **2017**, *208*, 673–681. [[CrossRef](#)]
15. Christensen, E.; Yanowitz, J.; Ratcliff, M.; McCormick, R.L. Renewable Oxygenate Blending Effects on Gasoline Properties. *Energy Fuels* **2011**, *25*, 4723–4733. [[CrossRef](#)]
16. Broustail, G.; Seers, P.; Halter, F.; Moréac, G.; Mounaim-Rousselle, C. Experimental determination of laminar burning velocity for butanol and ethanol iso-octane blends. *Fuel* **2011**, *90*, 1–6. [[CrossRef](#)]
17. Bogin, G.E., Jr.; Luecke, J.; Ratcliff, M.A.; Osecky, E.; Zigler, B.T. Effects of iso-octane/ethanol blend ratios on the observance of negative temperature coefficient behavior within the Ignition Quality Tester. *Fuel* **2016**, *186*, 82–90. [[CrossRef](#)]
18. Barraza-Botet, C.L.; Wooldridge, M.S. Combustion chemistry of iso-octane/ethanol blends: Effects on ignition and reaction pathways. *Combust. Flame* **2018**, *188*, 324–336. [[CrossRef](#)]
19. Foong, T.M.; Morganti, K.J.; Brear, M.J.; da Silva, G.; Yang, Y.; Dryer, F.L. The octane numbers of ethanol blended with gasoline and its surrogates. *Fuel* **2014**, *115*, 727–739. [[CrossRef](#)]
20. Schifter, I.; González, U.; González-Macías, C. Effects of ethanol, ethyl-tert-butyl ether and dimethyl-carbonate blends with gasoline on SI engine. *Fuel* **2016**, *183*, 253–261. [[CrossRef](#)]
21. Chan, J.H.; Tsolakis, A.; Herreros, J.M.; Kallis, K.X.; Hergueta, C.; Sittichompoo, S.; Bogarra, M. Combustion, gaseous emissions and PM characteristics of Di-Methyl Carbonate (DMC)-gasoline blend on gasoline Direct Injection (GDI) engine. *Fuel* **2020**, *263*, 116742. [[CrossRef](#)]
22. Wagner, C.; Keskin, M.-T.; Pitsch, H.; Grill, M.; Bargende, M.; Cai, L. Potential Analysis and Virtual Development of SI Engines Operated with Synthetic Fuel DMC+. SAE Technical Paper 2020-01-0342. 2020. Available online: <https://www.sae.org/publications/technical-papers/content/2020-01-0342/> (accessed on 23 October 2023).
23. Chen, G.; Yu, W.; Fu, J.; Huang, J.M.Z.; Yang, J.; Wang, Z.; Jin, H.; Qi, F. Experimental and modeling study of the effects of adding oxygenated fuels to premixed n-heptane flames. *Combust. Flame* **2012**, *159*, 2324–2335. [[CrossRef](#)]
24. Gao, Z.; Hu, E.; Xu, Z.; Huang, S.; Ku, J.; Huang, Z. Measurements and kinetic study on the ignition delay time of dimethyl carbonate/n-heptane/oxygen/argon mixtures. *Combust. Sci. Technol.* **2018**, *190*, 933–948. [[CrossRef](#)]
25. Tan, Y.R.; Salamanca, M.; Bai, J.; Akroyd, J.; Kraft, M. Structural effects of C<sub>3</sub> oxygenated fuels on soot formation in ethylene coflow diffusion flames. *Combust. Flame* **2021**, *232*, 111512. [[CrossRef](#)]
26. Pacheco, M.A.; Marshall, C.L. Review of Dimethyl Carbonate (DMC) Manufacture and Its Characteristics as a Fuel Additive. *Energy Fuels* **1997**, *11*, 2–29. [[CrossRef](#)]
27. Takahashi, E.; Nagano, Y.; Kitagawa, T.; Nishioka, M.; Nakamura, T.; Nakano, M. Demonstration of knock intensity mitigation through dielectric barrier discharge reformation in an RCEM. *Combust. Flame* **2020**, *216*, 185–193. [[CrossRef](#)]
28. Takahashi, E.; Kuramochi, A.; Nishioka, M. Turbulent flame propagation enhancement by application of dielectric barrier discharge to fuel-air mixtures. *Combust. Flame* **2018**, *192*, 401–409. [[CrossRef](#)]
29. Takahashi, E.; Sakamoto, S.; Imamura, O.; Ohkuma, Y.; Yamasaki, H.; Furutani, H.; Akihama, K. Fundamental characteristics of laser breakdown assisted long distance discharge ignition. *J. Phys. D Appl. Phys.* **2019**, *52*, 485501. [[CrossRef](#)]
30. Takahashi, E.; Kato, S. Laser ablation ignition of flammable gas. *Jpn. J. Appl. Phys.* **2021**, *60*, 047001. [[CrossRef](#)]
31. Vipavanich, C.; Chuepeng, S.; Skullong, S. Heat release analysis and thermal efficiency of a single cylinder diesel dual fuel engine with gasoline port injection. *Case Stud. Therm. Eng.* **2018**, *12*, 143–148. [[CrossRef](#)]
32. Heywood, J.B. *Internal Combustion Engine Fundamentals*; McGraw-Hill Education: New York, NY, USA, 1988; pp. 372–373,382.
33. Han, W.-Q.; Yao, C.-D. Research on high cetane and high octane number fuels and the mechanism for their common oxidation and auto-ignition. *Fuel* **2015**, *150*, 29–40. [[CrossRef](#)]
34. Boot, M.D.; Tian, M.; Hensen, E.J.M.; Sarathy, S.M. Impact of fuel molecular structure on auto-ignition behavior—Design rules for future high performance gasolines. *Prog. Energy Combust. Sci.* **2017**, *60*, 1–25. [[CrossRef](#)]
35. Yang, B.; Sun, W.; Moshhammer, K.; Hansen, N. Review of the Influence of Oxygenated Additives on the Combustion Chemistry of Hydrocarbons. *Energy Fuels* **2021**, *35*, 13550–13568. [[CrossRef](#)]

36. Kanayama, K.; Takahashi, S.; Morikura, S.; Nakamura, H.; Tezuka, T.; Maruta, K. Study on oxidation and pyrolysis of carbonate esters using a micro flow reactor with a controlled temperature profile. Part I: Reactivities of dimethyl carbonate, ethyl methyl carbonate and diethyl carbonate. *Combust. Flame* **2022**, *237*, 111810. [[CrossRef](#)]
37. Marinov, N.M. A Detailed Chemical Kinetic Model for High Temperature Ethanol Oxidation. *Int. J. Chem. Kinet.* **1999**, *31*, 183–220. [[CrossRef](#)]
38. Glaude, P.A.; Pitz, W.J.; Thomson, M.J. Chemical kinetic modeling of dimethyl carbonate in an opposed-flow diffusion flame. *Proc. Combust. Inst.* **2005**, *30*, 1111–1118. [[CrossRef](#)]
39. Rau, F.; Hartl, S.; Voss, S.; Still, M.; Hasse, C.; Trimis, D. Laminar burning velocity measurements using the Heat Flux method and numerical predictions of iso-octane/ethanol blends for different preheat temperatures. *Fuel* **2015**, *140*, 10–16. [[CrossRef](#)]
40. Mannaa, O.A.; Mansour, M.S.; Roberts, W.L.; Chung, S.H. Laminar Burning Velocities of Fuels for Advanced Combustion Engines (FACE) Gasoline and Gasoline Surrogates with and without Ethanol Blending Associated with Octane Rating. *Combust. Sci. Technol.* **2016**, *188*, 692–706. [[CrossRef](#)]
41. Burluka, A.A.; Gaughan, R.G.; Griffiths, J.F.; Mandilas, C.; Sheppard, C.G.W.; Woolley, R. Turbulent burning rates of gasoline components, Part 1—Effect of fuel structure of C<sub>6</sub> hydrocarbons. *Fuel* **2016**, *167*, 347–356. [[CrossRef](#)]
42. Li, Z.; Han, W.; Liu, D.; Chen, Z. Laminar flame propagation and ignition properties of premixed iso-octane/air with hydrogen addition. *Fuel* **2015**, *158*, 443–450. [[CrossRef](#)]
43. Baloo, M.; Dariani, B.M.; Akhlaghi, M.; Chitsaz, I. Effect of iso-octane/methane blend on laminar burning velocity and flame instability. *Fuel* **2015**, *144*, 264–273. [[CrossRef](#)]
44. Petrakides, S.; Chen, R.; Gao, D.; Wei, H. Experimental Investigation on the Laminar Burning Velocities and Markstein Lengths of Methane and PRF95 Dual Fuels. *Energy Fuels* **2016**, *30*, 6777–6789. [[CrossRef](#)]

**Disclaimer/Publisher’s Note:** The statements, opinions and data contained in all publications are solely those of the individual author(s) and contributor(s) and not of MDPI and/or the editor(s). MDPI and/or the editor(s) disclaim responsibility for any injury to people or property resulting from any ideas, methods, instructions or products referred to in the content.